

A Novel Compound ARN-3236 Inhibits Salt-Inducible Kinase 2 and Sensitizes Ovarian Cancer Cell Lines and Xenografts to Paclitaxel

Jinhua Zhou^{1,2}, Albandri Alfraidi¹, Shu Zhang¹, Janice M. Santiago-O'Farrill¹, Venkata Krishna Yerramreddy Reddy³, Abdulkhaliq Alsaadi⁴, Ahmed A. Ahmed⁴, Hailing Yang¹, Jinsong Liu⁵, Weiqun Mao¹, Yan Wang¹, Hiroshi Takemori⁶, Hariprasad Vankayalapati³, Zhen Lu¹, and Robert C. Bast Jr¹

Abstract

Purpose: Salt-inducible kinase 2 (SIK2) is a centrosome kinase required for mitotic spindle formation and a potential target for ovarian cancer therapy. Here, we examine the effects of a novel small-molecule SIK2 inhibitor, ARN-3236, on sensitivity to paclitaxel in ovarian cancer.

Experimental Design: SIK2 expression was determined in ovarian cancer tissue samples and cell lines. ARN-3236 was tested for its efficiency to inhibit growth and enhance paclitaxel sensitivity in cultures and xenografts of ovarian cancer cell lines. SIK2 siRNA and ARN-3236 were compared for their ability to produce nuclear-centrosome dissociation, inhibit centrosome splitting, block mitotic progression, induce tetraploidy, trigger apoptotic cell death, and reduce AKT/survivin signaling.

Results: SIK2 is overexpressed in approximately 30% of high-grade serous ovarian cancers. ARN-3236 inhibited the

growth of 10 ovarian cancer cell lines at an IC₅₀ of 0.8 to 2.6 μmol/L, where the IC₅₀ of ARN-3236 was inversely correlated with endogenous SIK2 expression (Pearson $r = -0.642$, $P = 0.03$). ARN-3236 enhanced sensitivity to paclitaxel in 8 of 10 cell lines, as well as in SKOv3ip ($P = 0.028$) and OVCAR8 xenografts. In at least three cell lines, a synergistic interaction was observed. ARN-3236 uncoupled the centrosome from the nucleus in interphase, blocked centrosome separation in mitosis, caused prometaphase arrest, and induced apoptotic cell death and tetraploidy. ARN-3236 also inhibited AKT phosphorylation and attenuated survivin expression.

Conclusions: ARN-3236 is the first orally available inhibitor of SIK2 to be evaluated against ovarian cancer in preclinical models and shows promise in inhibiting ovarian cancer growth and enhancing paclitaxel chemosensitivity. *Clin Cancer Res*; 23(8):1945–54. ©2016 AACR.

Introduction

Ovarian cancer is one of the most lethal malignancies. The survival of ovarian cancer patients depends critically on response to platinum- and taxane-based chemotherapy. Whereas 70% of ovarian cancers respond to platinum derivatives,

only approximately 40% of patients undergo objective regression following treatment with paclitaxel (1). Improved outcomes might be attained if sensitivity to paclitaxel was enhanced. Several attempts have been made to reverse mechanisms of acquired taxane resistance, but less attention has been given to enhancing sensitivity to taxanes during primary treatment of ovarian cancer, especially high-grade serous ovarian cancer (2–5).

In earlier studies, we had undertaken an siRNA screen to identify kinases that regulate sensitivity to paclitaxel (6). One of the most promising candidates to emerge from that screen was salt-inducible kinase 2 (SIK2), a serine/threonine kinase, which is required for bipolar mitotic spindle formation and normal mitotic progression (7). Consequently, SIK2 presents an attractive therapeutic target for ovarian cancer treatment (7).

Here, we report that a novel 1H-(pyrazol-4-yl)-1H-pyrrolo[2,3-b]pyridine small-molecule inhibitor of SIK2 (ARN-3236) [16] inhibits ovarian cancer cell growth and sensitizes ovarian cancer cells and xenografts to paclitaxel by inhibiting centrosome splitting and AKT/survivin signaling.

Materials and Methods

Tissue microarray

A formalin-fixed, paraffin-embedded tissue microarray (TMA) that contained samples of 193 primary serous ovarian cancers

¹Department of Experimental Therapeutics, The University of Texas MD Anderson Cancer Center, Houston, Texas. ²Department of Obstetrics and Gynecology, The First Affiliated Hospital of Soochow University, Suzhou, China. ³Arrien Pharmaceuticals, Salt Lake City, Utah. ⁴The Nuffield Department of Obstetrics and Gynecology, University of Oxford, Oxford, United Kingdom. ⁵Department of Pathology, The University of Texas MD Anderson Cancer Center, Houston, Texas. ⁶National Institutes of Biomedical Innovation, Health and Nutrition (NIBIOHN), Ibaraki, Osaka, Japan.

Note: Supplementary data for this article are available at Clinical Cancer Research Online (<http://clincancerres.aacrjournals.org/>).

J. Zhou and A. Alfraidi contributed equally to this article.

H. Vankayalapati, Z. Lu, and R.C. Bast share senior authorship.

Corresponding Author: Robert C. Bast Jr, Department of Experimental Therapeutics, The University of Texas MD Anderson Cancer Center, 1400 Pressler Street, FCT 8.5066, Houston, TX 77030. Phone: 713-792-7743; Fax: 713-792-2107; E-mail: rbast@mdanderson.org

doi: 10.1158/1078-0432.CCR-16-1562

©2016 American Association for Cancer Research.

Translational Relevance

Ovarian cancer is the fifth leading cause of death from cancer. More than half of ovarian cancers are resistant to paclitaxel at the time of diagnosis. Salt-inducible kinase 2 (SIK2) is overexpressed in 30% of ovarian cancers and regulates mitotic progression. Here, we have shown that a novel SIK2 inhibitor, ARN-3236, blocks the activity of SIK2 kinase and inhibits ovarian cancer cell growth, enhancing the paclitaxel sensitivity. Similar to the effect of SIK2 knockdown with siRNA, ARN-3236 induced apoptotic cell death by inhibiting AKT/survivin signaling. In addition, ARN-3236 induced G₂-M arrest and mitotic catastrophe in ovarian cancer cells. Thus, ARN-3236 appears to be a drug with promise for enhancing primary treatment of ovarian cancers.

(183 cases of high grade and 10 cases of low grade) was obtained from the MD Anderson Pathology Department (MD Anderson Cancer Center, Houston, TX). Additional details are provided in Supplementary Table S1. The protocols for handling paraffin-embedded ovarian cancer specimens and analyzing patient data were approved by the ethical committees of the MDACC Institutional Review Boards. TMA construction was performed as described previously (8).

Growth inhibition assay

Cells were seeded in 96-well cell culture plates in triplicate and incubated for 16 hours. Then, cells were treated with DMSO or ARN-3236 for 24 hours, followed by an additional 72-hour incubation with paclitaxel at the concentration indicated. The sulforhodamine B (SRB) assay was used to measure the growth inhibition of each cell line with and without treatment as described previously (9). The concentration producing 50% growth inhibition (IC₅₀) was calculated by the following formula: $100 \times (T - T_0) / (C - T_0) = TC_{50}$, in which *T* is the optical density (OD) value after drug treatment, *T*₀ is the OD value at time 0, and *C* is the OD value for the diluent treatment (10). GraphPad Prism 5 software was used to generate growth curves. For studies of ARN-3236 and paclitaxel in combination, four groups were evaluated: (i) drug-free control; (ii) ARN-3236 alone; (iii) paclitaxel alone; and (iv) a combination of ARN-3236 and paclitaxel at 9 different concentrations (0, 0.2, 0.39, 0.78, 1.56, 3.13, 6.25, 12.5, and 25 μmol/L) of paclitaxel were used. To evaluate additive or synergistic interactions, a combination index (CI value) was calculated with CalcuSyn software (Biosoft), which was developed on the basis of the median effect principle of Chou–Talalay method (11). Values less than 1 were considered synergistic and those equal to 1 were additive.

Cell lines and cultures

HEY and A2780 human ovarian cancer cell lines were purchased from the ATCC. UPN251, OVCAR3, OVCAR5, OVCAR8, ES-2, OC316, SKOV3, and IGROV1 were kindly provided by Dr. Gordon Mills' laboratory (12–15), and all the cell lines were confirmed with STR DNA fingerprinting, which was performed by the MDACC Characterized Cell Line Core (supported by NCI CCSG # CA016672). SKOV3-SIK2 cell line was kindly provided by Dr. Ahmed's laboratory (16). SKOV3 and SKOV3-SIK2 cells were

cultured in McCoy's 5A medium; OVCAR3, OVCAR5, OVCAR8, HEY, OC316, A2780, IGROV1, ES-2, and UPN251 cells were cultured in RPMI1640 medium. All media were obtained from the Media Preparation Core Facility at MD Anderson Cancer Center. All cell lines were tested for mycoplasma with a MycoSensor PCR Assay Kit from Stratagene (cat. 302109) and found to be free from contamination.

siRNA transfection

The siGenome siRNAs (Dharmacon) were used to target individual genes for inhibiting their expression as described previously (7). Cells were transfected with a negative control siRNA or a specific siRNA using DharmaFECT 4 reagent (Dharmacon). A mixture of siRNA (25 nmol/L final concentration) and DharmaFECT 4 reagent was incubated for 20 minutes at room temperature before being applied to the cells.

Nuclear centrosome uncoupling

The distance from the nucleus to the centrosome was measured as described previously (7), and details regarding staining and measurement are provided in Supplementary Methods.

Counting mitotic cells and mitotic cell polarity

After treatment, cells were fixed and stained using anti-γ-tubulin and anti-phospho-histone H3 antibodies. DAPI was used for nuclear staining. The percentage of mitotic cells was calculated using the following formula: (phosphor-histone H3-positive cells/DAPI-positive cells) × 100%. Mitotic cell polarity was determined as described previously (7). Additional detailed information is provided in Supplementary Methods.

Reverse-phase protein array

SKOV3 cells were treated with ARN-3236 (2 μmol/L) or DMSO diluent for 48 hours. Reverse-phase protein array (RPPA) analysis was performed at the MD Anderson Cancer Center RPPA Core Facility. Additional information is provided in the Supplementary Methods.

Human ovarian cancer xenografts in nude mice

Female athymic nu/nu mice were used to determine the anti-cancer effect of ARN-3236. Experiments using Nu/Nu mice were reviewed and approved by the Institutional Animal Care and Use Committee (IACUC ID: 00001052-RN00; MD Anderson Cancer Center, Houston, TX). SKOV3ip1 and OVCAR8 cells were injected intraperitoneally. ARN-3236 was administered orally at a dose of 60 mg/kg/day for 7 days. Paclitaxel was administered intraperitoneally once a week at a dose of 5 mg/kg in SKOV3ip cells and 1 mg/kg in OVCAR8 cells. On day 7 after cancer cell injection, the mice were randomly assigned to the following treatment groups (*n* = 6 mice per group): (i) nontreatment control; (ii) vehicle control for ARN-3236; (iii) ARN-3236; (iv) paclitaxel; and (v) combination of paclitaxel and ARN-3236. SKOV3ip-bearing mice were treated for 3 weeks, and OVCAR8-bearing mice were treated for 4 weeks. After treatment, mice were sacrificed by CO₂ at the end of the studies. All tumors were collected immediately after death and weighed.

Statistical analysis

Data are expressed as mean ± SD. We used SPSS23.0 Software to calculate statistical significance between groups. GraphPad

Prism 6.0 was used for multiple comparison tests. $P < 0.05$ was considered as statistically significant.

More details of experiments are listed in Supplementary Methods.

Results

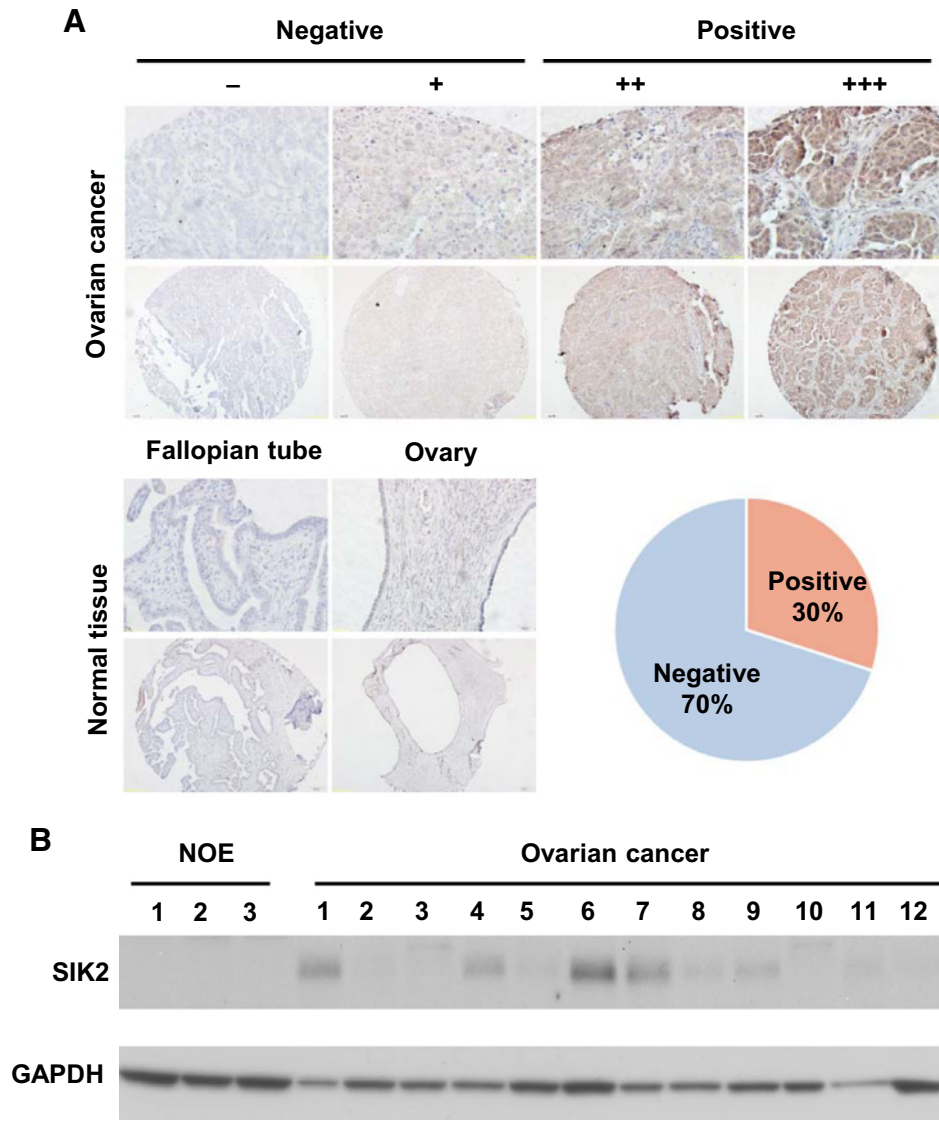
SIK2 is overexpressed in 30% of serous ovarian cancers

To determine SIK2 expression in epithelial ovarian cancer, a cohort of 193 serous ovarian cancers and 60 normal ovarian tissues and normal fallopian tube specimens were analyzed for SIK2 protein expression by IHC. Positive SIK2 staining was observed in about 30% of ovarian cancers in comparison with negative staining in normal ovarian surface epithelial cells and normal fallopian epithelial cells (Fig. 1A). In addition, SIK2 protein was elevated in five of 12 high-grade serous ovarian cancer tumor cell lysates compared with normal ovarian epithelium cell lysates (Fig. 1B). Thus, SIK2 is strongly expressed in 30% of human ovarian cancer and may serve as a potential therapeutic target.

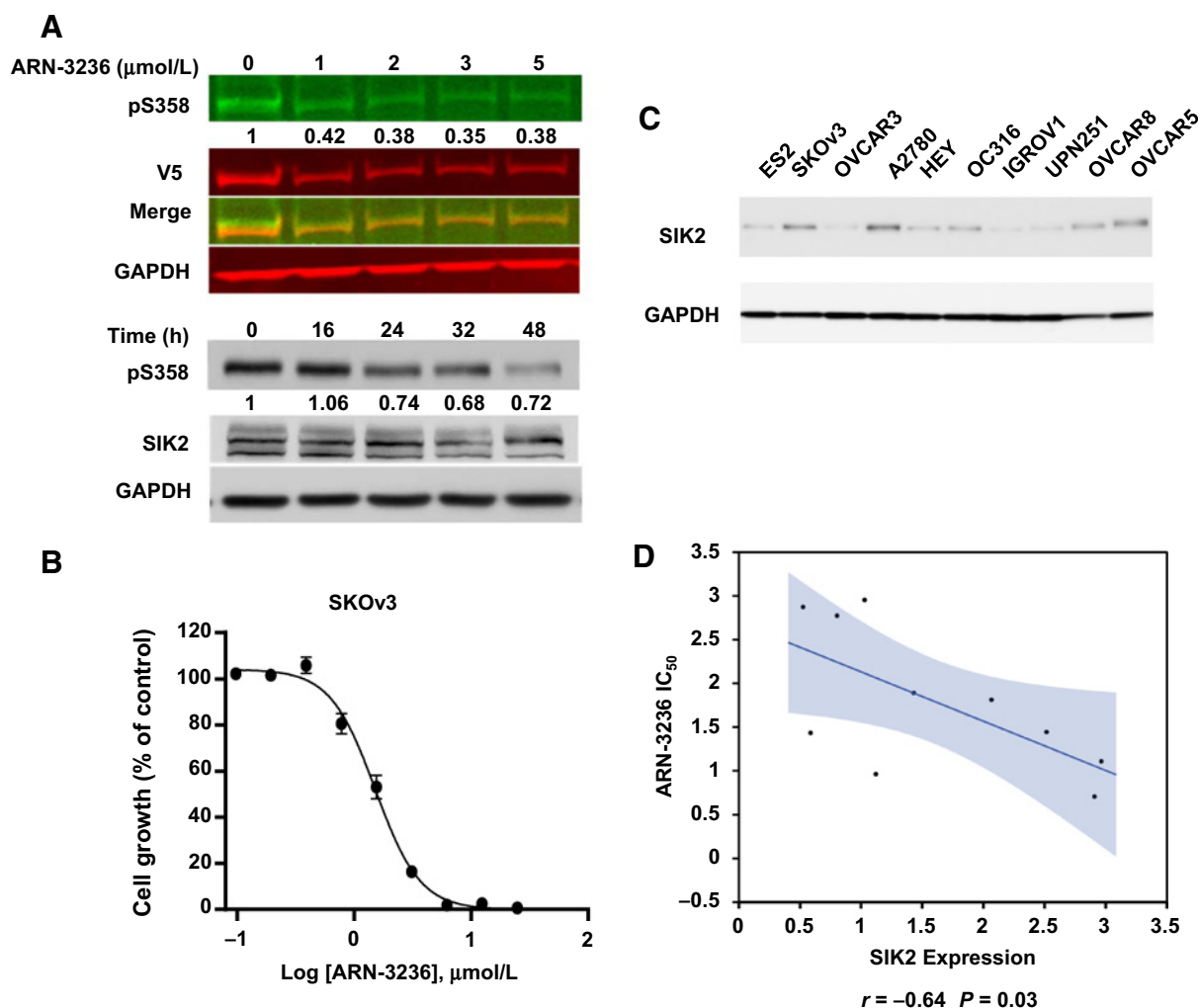
ARN-3236 inhibits SIK2 kinase activity

Previously, we have shown that SIK2 plays a key role in the progression of mitosis and in regulating paclitaxel sensitivity by knocking down SIK2 protein with siRNA (7). Given the challenges of delivering siRNA to cancer cells *in vivo*, we had sought orally available small-molecule inhibitors of SIK2 to enhance the chemosensitivity of ovarian cancers. Arrien Pharmaceuticals has developed a novel 1H-(pyrazol-4-yl)-1H-pyrrolo[2,3-b]pyridine inhibitor, ARN-3236 (17), which competes with ATP binding to SIK2 protein and inhibits SIK2 kinase activity (18, 19). Previous publications have shown that ARN-3236 inhibits SIK2 activity with an $IC_{50} < 1$ nmol/L but does not significantly inhibit the other two SIK family members SIK1 and SIK3 as well as other AMP-activated protein kinase (AMPK) family members (19). We tested the inhibitory effect of ARN-3236 using TORC2 (transducer of regulated CREB protein 2)-derived peptide, a direct substrate of SIK2 with a phosphorylation consensus sequence LX[HKR]S/TXSXXXL (aa166-175; ref. 20) and demonstrated that ARN-3236 diminished TORC2

Figure 1. SIK2 is overexpressed in 30% of serous ovarian cancers. **A**, Representative images of human ovarian tumors with low or high immunohistochemical staining for SIK2, and the percentage of SIK2-positive (+) and SIK2-negative (–) samples. **B**, Lysates from three cases of normal ovarian epithelium and 12 cases of primary serous ovarian cancer tissue were subjected to immunoblotting analysis for SIK2 expression.



Zhou et al.

**Figure 2.**

ARN-3236 inhibits SIK2 kinase activity and ovarian cancer cell growth. **A**, SKOV3-SIK2 cells were treated with ARN-3236 at the indicated concentrations for 24 hours, or SKOV3-SIK2 cells were treated with ARN3236 at a final concentration of 2 μmol/L for the indicated time periods. Cell lysates were collected and analyzed by Western blot analysis for SIK2-pS358 and total protein level of SIK2. The numbers below the bands are intensities of pS358 normalized to GAPDH. **B**, SKOV3 cells were plated at a density of 8,000/well in 96-well plates, then treated with ARN-3236 or DMSO for 72 hours, and cell viability was measured with an SRB assay. **C**, Endogenous SIK2 expression was detected by Western blot analysis in indicated ovarian cancer cell lines. **D**, The correlation between endogenous SIK2 expression and IC₅₀ value in each cell line was plotted.

phosphorylation in a dose-dependent manner (Supplementary Fig. S1A). To examine the pharmacodynamics of ARN-3236, we studied S358 autophosphorylation of SIK2, which has been correlated with SIK2 activity (16). We confirmed that ARN-3236 blocked autophosphorylation of SIK2 and decreased SIK2 activity in ovarian cancer cells in a dose-dependent and a time-dependent manner (Fig. 2A). Thus, ARN-3236 is a potent and specific SIK2 kinase inhibitor.

ARN-3236 inhibits cell growth and increases paclitaxel sensitivity in ovarian cancer cells

To determine whether ARN-3236 could inhibit growth of ovarian cancer cells, the effect of ARN-3236 was measured in 10 ovarian cancer cell lines using short-term cell proliferation assays, and the IC₅₀ of ARN-3236 was calculated in each cell line. Significant inhibition was achieved in all cell lines. The

IC₅₀ values of ES2, SKOV3, OVCAR3, A2780, HEY, OC316, IGROV1, UPN251, OVCAR8, and OVCAR5 cells were 1.22, 1.23, 2.58, 0.93, 0.8, 1.63, 2.51, 2.42, 1.56, and 1.19 μmol/L, respectively. Thus, the IC₅₀ ranged from 0.8 to 2.6 μmol/L (Fig. 2B and Supplementary Fig. S1B–S1J). Endogenous SIK2 protein expression correlated inversely with the IC₅₀ value of ARN-3236 in these cancer cell lines (Pearson $r = -0.642$, $P = 0.03$; Fig. 2C and D), indicating the cells with relatively high expression of SIK2 protein are more sensitive to treatment with the SIK2 inhibitor. The ability of ARN-3236 to sensitize ovarian cancer cells to paclitaxel was documented in eight ovarian cancer cell lines, including OC316, OVCAR8, SKOV3, A2780, OVCAR5, HEY, ES2, and UPN251, where treatment with ARN-3236 produced a >1.5-fold change in IC₅₀ (Fig. 3A and B and Supplementary Fig. S2A–S2F). Sensitization to paclitaxel was not observed in OVCAR3 and IGROV1 (Supplementary

Figure 3.

ARN-3236 increases paclitaxel sensitivity in ovarian cancer cells *in vitro* and *in vivo*. **A** and **B**, OC316 and OVCAR8 cells were plated at a density of 8,000/well in a 96-well plate, then sequentially treated with ARN-3236 or DMSO for 24 hours and with increasing concentrations of paclitaxel (PTX) for another 72 hours. Cell viability was measured with an SRB assay. **C**, Flow diagram showing the design of the *in vivo* experiment. **D**, SKOV3ip cancer cells were inoculated intraperitoneally into nu/nu mice and treated as indicated in the Materials and Methods section. After treatment (Tx), mice were sacrificed and the tumors weighed. The tumor weight of individual mice in each group is plotted ($n = 6$ in each group). *, $P < 0.05$.

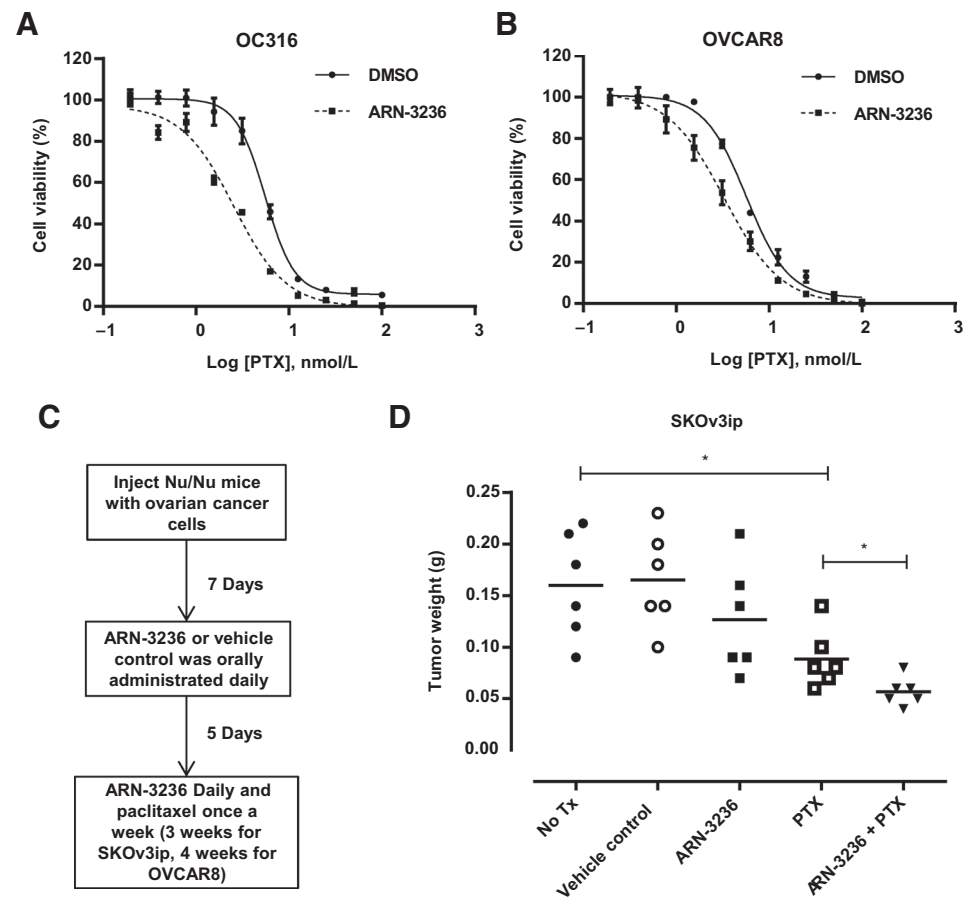


Fig. S2G and S2H) that exhibited relatively low expression level of SIK2 protein. In addition, ARN-3236 and paclitaxel combination study in SKOV3, OC126, and OVCAR8 cell lines further confirmed that treatment of ARN-3236 with paclitaxel provide synergistic effect (Supplementary Fig. S2J). Thus, ARN-3236 increased sensitivity to paclitaxel in cell lines with relatively high expression of SIK2.

ARN-3236 sensitizes ovarian cancer to paclitaxel *in vivo*

The antitumor activity of ARN-3236 was measured using ovarian cancer xenograft model in nu/nu mice (Fig. 3C). In SKOV3ip xenograft model, ARN-3236 plus paclitaxel produced greater inhibition of tumor growth than any other group and showed statistically significant difference compared with paclitaxel alone ($P = 0.028$; Fig. 3D). A combination of ARN-3236 with paclitaxel produced a similar trend in growth inhibition in a xenograft model using OVCAR8 high-grade serous ovarian cancer cells, where significant inhibition ($P = 0.02$) was observed only with the combined treatment (Supplementary Fig. S2I). Together, these data confirm that ARN-3236 inhibits SIK2 activity and enhances paclitaxel sensitivity not only in cultured cells but also in ovarian cancer xenografts, suggesting the potential of ARN-3236 in improving chemotherapy efficiency in ovarian cancers.

ARN-3236 increases centrosome uncoupling from nucleus

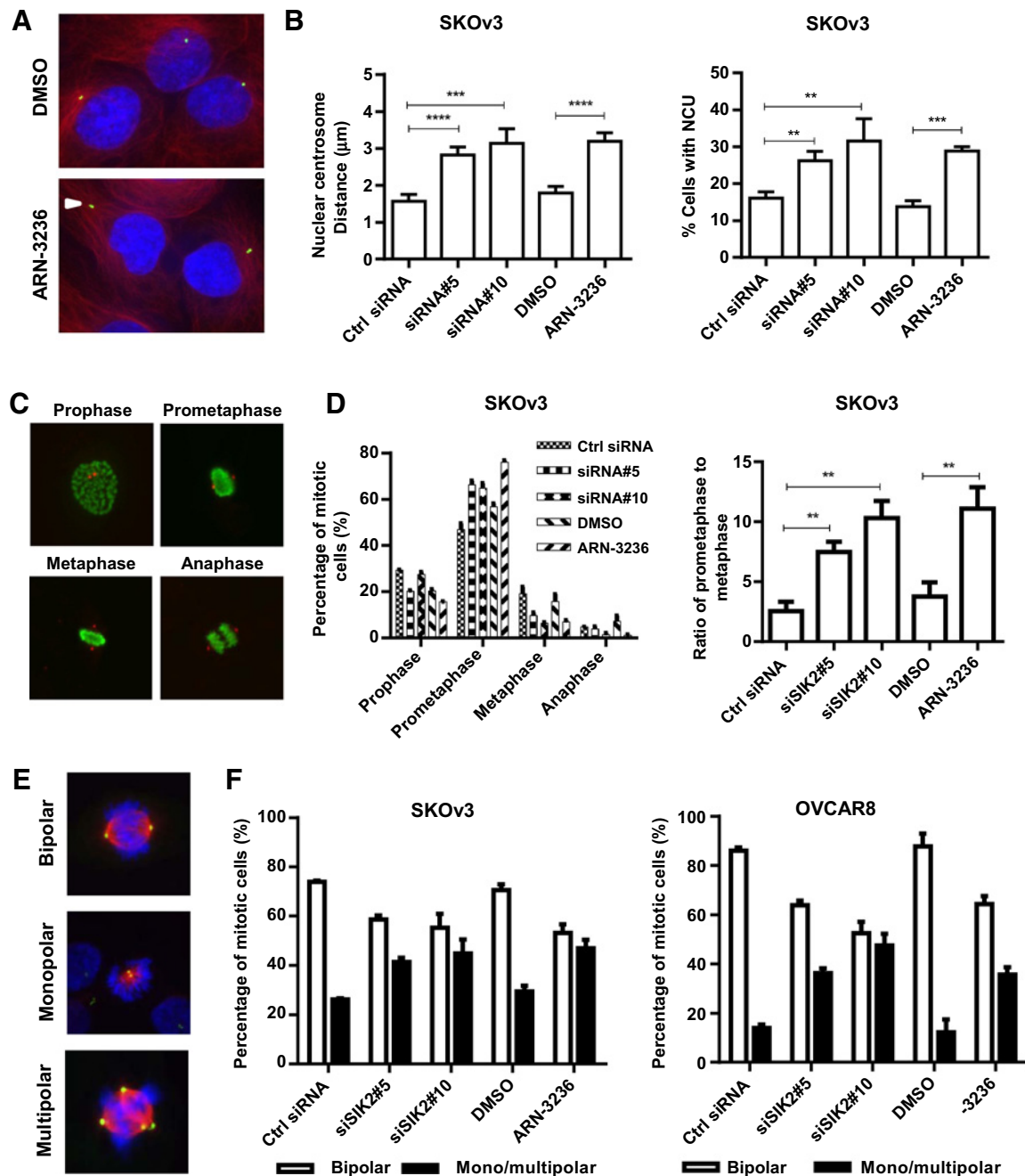
The centrosome, located close to the nuclear envelope during interphase, is an organelle that serves as the microtubule-orga-

nizing center for cells as well as a regulator of cell-cycle progression. SIK2 knockdown resulted in nuclear-centrosome uncoupling (NCU; nuclear centrosome distance of $>2 \mu\text{m}$; ref. 7). To test the effect of ARN-3236 on centrosome uncoupling, nuclear centrosome distance was measured in SKOV3 and A2780 cells after treatment of ARN-3236 for 48 hours. ARN-3236 treatment increased the nuclear centrosome distance from 1.790 to 3.198 μm in SKOV3 cells and from 1.410 to 2.230 μm in A2780 cells ($P < 0.0001$; Fig. 4A and B and Supplementary Fig. S3A), suggesting that the SIK2 inhibitor abolished this centrosome function. In addition, a significant increase in the percentage of NCU-positive cells was also detected after SIK2 inhibitor treatment compared with control (30.0%–15.2% in SKOV3 cells, 37.6%–18.7% in A2780 cells, respectively, $P < 0.01$; Fig. 4B and Supplementary Fig. S3A). Thus, ARN-3236 interfered with the appropriate centrosome positioning in interphase.

ARN-3236 inhibits centrosome splitting in mitotic cells

Mitosis is a continuous process that passes through different stages: prophase, prometaphase, metaphase, anaphase, and telophase. In early mitosis, separation of centrosomes is driven by several motor proteins with the onset of prophase to ensure spindle bipolarity (21, 22). Previously, we reported that SIK2 regulates centrosome splitting, and SIK2 knockdown resulted in centrosome splitting failure and mitotic catastrophe (7, 23). To determine whether ARN-3236 blocks centrosome function in mitotic cells, we calculated the percentage of each phase in mitotic cells after ARN-3236 treatment. We have shown that

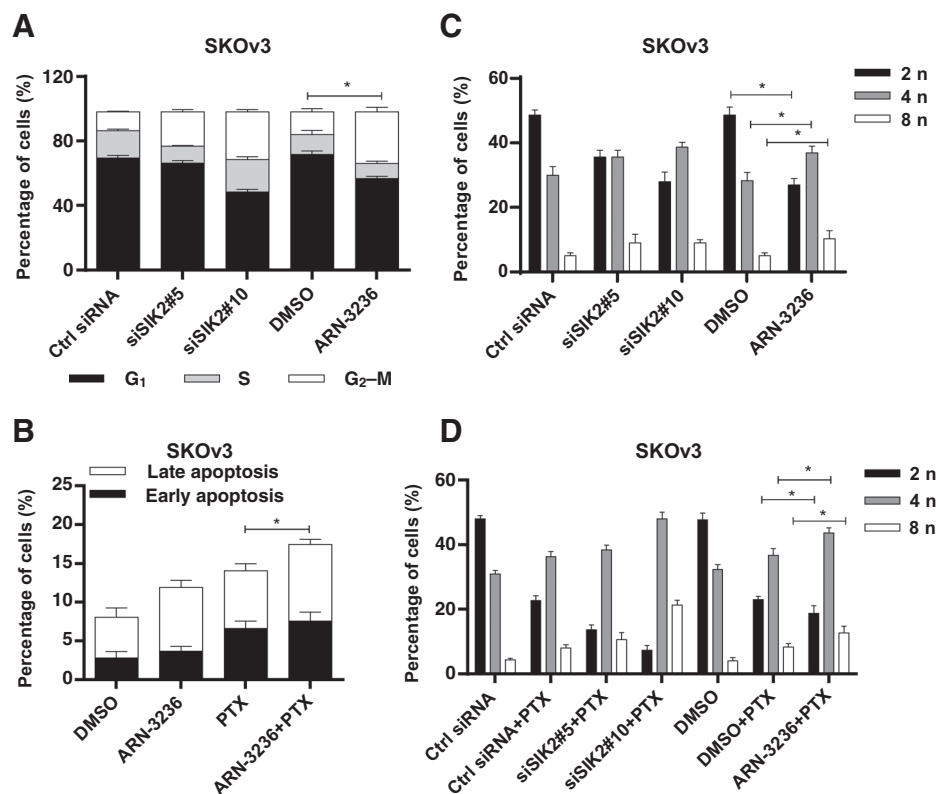
Zhou et al.

**Figure 4.**

ARN-3236 uncouples the centrosome from the nucleus and inhibits centrosome separation. **A**, Shown is a representative centrosome localization in relation to the nucleus 48 hours after DMSO or ARN-3236 treatment. DAPI, blue; α -tubulin, red; γ -tubulin, green; arrowhead, dislocated centrosome. **B**, SKOV3 cells were plated on coverslips and transfected with siRNA or treated with DMSO or ARN-3236 (1 $\mu\text{mol/L}$); 48 hours following treatment, the distance from the centrosome to the nuclear envelop in each cell was measured, and the percentage of cells showing NCU was calculated. The bar plots show the mean \pm SD of the distance in microns (left plot) and the mean \pm SD of the percentage of cells with NCU from three independent experiments (right plot). **C**, Cells were treated as in **B** and stained using anti- γ -tubulin (red) and anti-phosphohistone H3 (green) to reveal the centrosome position in mitosis in relation to chromosomes. Shown are the representative examples of different mitosis phases in control (Ctrl) cells. **D**, After the same treatment as in **B**, mitotic cells at each stage were counted and plotted. Bar plots represent the mean \pm SD of the percentage of cells at different stages of mitosis (left plot) and the mean prometaphase/metaphase ratio \pm SD (right plot). **E**, Cells were treated as in **B** and stained using anti- γ -tubulin (green), α -tubulin (red), and DAPI to reveal the centrosome position in relation to chromosomes. Shown are the representative examples of bipolar and mono/multipolar mitotic cells. **F**, After the same treatment as in **B**, bipolar and mono/multipolar mitotic cells were counted and plotted. Bar plots represent the mean \pm SD of the percentage of bipolar and mono/multipolar mitotic cells. **, $P < 0.01$; ***, $P < 0.001$; ****, $P < 0.0001$.

Figure 5.

ARN-3236 induces cell-cycle arrest, apoptosis, and tetraploidy. **A**, SKOV3 cells were transfected with SIK2 siRNA or treated with ARN-3236 (1 μ mol/L) for 48 hours. After treatment, cells were fixed, stained with PI, and subjected to cell-cycle analysis. Ctrl, control. **B**, SKOV3 cells were treated with ARN-3236 (1 μ mol/L) for 24 hours and with paclitaxel (PTX; 3 nmol/L) for another 72 hours, then were stained with Annexin V-FITC/PI and subjected to apoptotic analysis. **C**, SKOV3 cells were treated with SIK2 siRNA or ARN-3236 (1 μ mol/L) for 48 hours, fixed, stained with PI, and subjected to cell ploidy analysis. The representative percentages of cell in 2n, 4n, and 8n are shown. **D**, SKOV3 cells were transfected with SIK2 siRNA or treated with ARN-3236 (1 μ mol/L) for 24 hours and with paclitaxel (3 nmol/L) for another 72 hours; then, cells were fixed, stained with PI, and subjected to cell ploidy analysis. The representative percentage of cell in 2n, 4n, and 8n is shown. All the experiments were repeated in triplicate. *, $P < 0.05$.



ARN-3236 induced accumulation of cells in prometaphase (Fig. 4C and D and Supplementary Fig. S3B and S3C) and increased the ratio of prometaphase to metaphase cells in mitosis, suggesting that ARN-3236 induces prometaphase arrest in ovarian cancer cells. Importantly, ARN-3236 decreased the percentage of bipolar mitotic cells and increased the percentage of monopolar/multipolar mitotic cells (Fig. 4E and F). These data indicate that ARN-3236 inhibits centrosome splitting in mitotic ovarian cancer cells.

ARN-3236 induces cell-cycle arrest, apoptosis, and tetraploidy

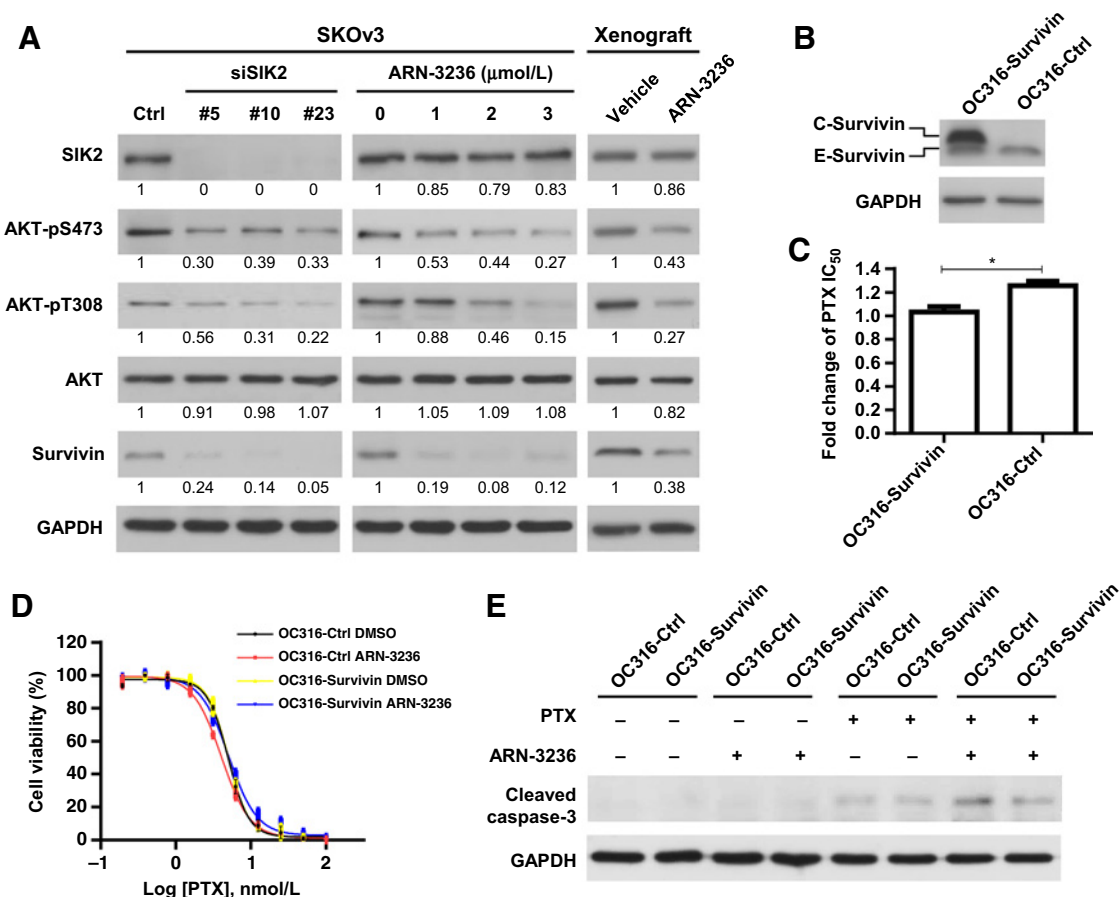
To confirm that the failure of centrosome splitting and the delay in mitotic progression induced by ARN-3236 can result in cell-cycle arrest and apoptosis, we first tested the effect of ARN-3236 on cell-cycle progression in ovarian cancer cells. Treatment with ARN-3236 induced G_2 -M arrest (Fig. 5A and Supplementary Fig. S4A). Furthermore, measurement of apoptosis by flow cytometry indicated that ARN-3236 induced apoptosis both alone and in combination with paclitaxel (Fig. 5B and Supplementary Fig. S4B). Previously, we have shown that SIK2 depletion increases the cell ploidy index (7). In our current study, ARN-3236 treatment resulted in the accumulation of tetraploid cells (4n and 8n; Fig. 5C), and sequential treatment of ARN-3236 and paclitaxel led to further accumulation of tetraploid cells (4n and 8n) compared with treatment of paclitaxel or ARN-3236 alone (Fig. 5D). Tetraploid cells are often associated with failing mitosis, which leads to the gross nuclear alterations that constitute the most prominent morphologic traits of mitotic catastrophe. Mitotic catastrophe also has been extensively used as a term to indicate cell death resulting from aberrant mitosis (24, 25). Altogether, the results suggest that ARN-3236 and/or paclitaxel treatment may

inhibit ovarian cancer growth and induce cell death through multiple mechanisms, including G_2 -M arrest, apoptosis, and mitotic catastrophe.

ARN-3236 attenuates the AKT/survivin pathway

To identify potential mechanisms underlying regulation of apoptosis by SIK2 inhibition, RPPAs were used to monitor changes in signaling pathways. We found that ARN-3236 significantly inhibited AKT activation (Supplementary Fig. S5A), which is consistent with the results obtained when SIK2 was silenced with siRNA (7). To validate results obtained with RPPA analysis, positive hits were confirmed by Western blot analysis. ARN-3236 inhibits AKT activation by reducing phosphorylation of serine 473 as well as threonine 308 (Fig. 6A and Supplementary Fig. S5B). Furthermore, ARN-3236 also reduces the expression of survivin (Fig. 6A and Supplementary Fig. S5B), a downstream target of AKT, which contributes to paclitaxel resistance in many cancers (26, 27), suggesting that SIK2 regulates ovarian cancer cell growth and paclitaxel resistance, at least in part, through AKT/survivin signaling. Importantly, the ARN-3236-mediated changes in AKT phosphorylation and survivin observed in cultured cells were also confirmed in ovarian cancer xenografts *in vivo* (Fig. 6A and Supplementary Fig. S5C). In addition, whether survivin overrides the proapoptotic function of ARN-3236 and paclitaxel was investigated in the cells engineered to overexpress survivin (Fig. 6B). As shown in Fig. 6C and D, ARN-3236 moderately but significantly sensitized OC316-control cells to paclitaxel (paclitaxel IC_{50} : 4.732–5.248 nmol/L in DMSO, 3.873–4.252 nmol/L in ARN-3236, IC_{50} fold change 1.22, $P < 0.01$) but did not sensitize an OC316 subline with forced expression of survivin (paclitaxel IC_{50} : 4.737–5.254 nmol/L in

Zhou et al.

**Figure 6.**

ARN-3236 attenuates the AKT/survivin pathway. **A**, SKOV3 cells were transfected with SIK2 siRNA or treated with ARN-3236 for 48 hours; cell lysates were collected and analyzed by Western blot analysis for AKT-pS473, AKT-pT308, AKT, and survivin expression (left); right, immunoblotting analysis of tumor lysates after the indicated treatment detecting AKT-pS473, AKT-pT308, AKT, and survivin. **B**, The vector expressed survivin (C-survivin) and endogenous survivin (E-survivin) were detected by Western blot analysis in the cell lines indicated. Ctrl, control. **C** and **D**, Ovarian cancer cells of the lines indicated were added to 96-well plates at a density of 8,000 cells/well and treated with DMSO or ARN-3236 (0.6 μmol/L) for 24 hours, followed by different concentrations of paclitaxel (PTX) for a subsequent 72 hours. Cell viability was measured by an SRB assay. Triplicate assays were performed. The fold change in paclitaxel IC₅₀ values after ARN-3236 treatment are plotted for each cell line in **C**, and the cell viability curves are shown in **D**. **E**, Ovarian cancer cells were treated with ARN-3236 (0.6 μmol/L) for 24 hours and/or with paclitaxel (4 nmol/L) for subsequent 72 hours; cell lysates were collected and subjected to Western blot analysis of activated caspase-3. *, $P < 0.05$.

DMSO, 4.613–5.5230 nmol/L in ARN-3236, $P = 0.73$). OC316-survivin cells also exhibited attenuated activation of caspase-3 after ARN-3236 and paclitaxel treatment (Fig. 6E). Thus, down-regulation of survivin expression and activation of apoptosis is at least partially responsible for ARN-3236-mediated paclitaxel sensitization.

Discussion

SIK2 is a member of a family of AMPKs, which was originally cloned from the adrenal gland of a salt-treated rat (28). SIK2 has been shown to function in diverse biological processes, including gluconeogenesis, neuronal survival, melanogenesis, hepatic steatosis, and centrosome splitting (7, 29–32). SIK2 is also implicated in the progression of cancer (7, 33–35). In addition, a fraction of ovarian cancers depends on the SIK2 kinase for maintenance of cell proliferation and chemoresis-

tance (7). Some 30% of ovarian cancers overexpress SIK2, associated with a trend toward poor prognosis. Selective inhibition of SIK2 kinase is a potentially important approach for the treatment of ovarian cancer.

ARN-3236 is an orally bioavailable SIK2 small-molecule inhibitor. ARN-3236 inhibits SIK2 activity with subnanomolar potency but does not significantly inhibit the other two SIK family members SIK1 and SIK3 (19). To our knowledge, ARN-3236 is the first and most potent SIK2 inhibitor reported to date. ARN-3236 inhibited the growth of 10 ovarian cancer cell lines with IC₅₀ values of 0.8 to 2.6 μmol/L. Importantly, the IC₅₀ of ARN-3236 was inversely correlated with endogenous SIK2 expression across 10 different cell lines. Consequently, we have identified a potential biomarker for susceptibility to SIK2 inhibition with this compound. In our current study, primary sensitivity to paclitaxel has been enhanced by treatment of ARN-3236. As less than half of ovarian cancer patients exhibit

primary sensitivity to paclitaxel, there is considerable room for improvement in primary treatment. ARN-3236 and its congeners could fill this unmet medical need. Inhibition of growth and enhancement of paclitaxel sensitivity was observed in 8 of 10 ovarian cancer cell lines (36), suggesting that the combination of ARN-3236 and paclitaxel might improve efficacy in a significant fraction of patients with this disease. In addition, our data suggest that inhibition of SIK2 enzyme activity can mimic the effects of siRNA-mediated knockdown of SIK2 protein with regards to cell-cycle changes, induction of polyploidy, uncoupling of centrosomes from the nucleus, centrosome splitting, growth inhibition, and enhanced sensitivity to paclitaxel, associated with decreased signaling through AKT.

Regulators of mitosis have been successfully targeted by ARN-3236 to enhance response to taxane chemotherapy. Centrosomes are complex cellular substructures that are dynamically regulated by a series of biochemical and morphologic changes that parallel the progression of cell cycle. In addition to organizing cytoplasmic microtubule arrays during interphase, centrosomes direct formation and positioning of bipolar mitotic spindle and thereby enable equal partitioning of the replicated genome, and impaired centrosome function may lead to chromosome missegregation and accumulation of tetraploid cells. Tetraploid cells are often associated with failing mitosis and mitotic catastrophe, which has been extensively used as a term to indicate cell death resulting from aberrant mitosis (37). Because the functional significance of centrosome has been described in a variety of solid tumors, including breast, prostate, colon, ovarian, and pancreatic cancer (37, 38), centrosome has become an important focus for cancer therapy development (39, 40). Here, we show that ARN-3236 with the known SIK2 inhibition disturbed SIK2-dependent centrosome positioning in interphase and blocked centrosome separation in mitosis, sensitizing ovarian cancers to paclitaxel in culture and in xenografts. We believe these data further confirmed that ARN-3236 has potential for enhancing primary treatment of ovarian cancers.

References

- Muggia FM, Braly PS, Brady MF, Sutton G, Niemann TH, Lentz SL, et al. Phase III randomized study of cisplatin versus paclitaxel versus cisplatin and paclitaxel in patients with suboptimal stage III or IV ovarian cancer: a gynecologic oncology group study. *J Clin Oncol* 2000;18:106–15.
- Coleman RL, Monk BJ, Sood AK, Herzog TJ. Latest research and treatment of advanced-stage epithelial ovarian cancer. *Nat Rev Clin Oncol* 2013;10:211–24.
- Yu Y, Gaillard S, Phillip JM, Huang TC, Pinto SM, Tessarollo NG, et al. Inhibition of spleen tyrosine kinase potentiates paclitaxel-induced cytotoxicity in ovarian cancer cells by stabilizing microtubules. *Cancer Cell* 2015;28:82–96.
- McGrail DJ, Khambhati NN, Qi MX, Patel KS, Ravikumar N, Brandenburg CP, et al. Alterations in ovarian cancer cell adhesion drive taxol resistance by increasing microtubule dynamics in a FAK-dependent manner. *Sci Rep* 2015;5:9529.
- Kurman RJ, Shih Ie M. The dualistic model of ovarian carcinogenesis: revisited, revised, and expanded. *Am J Pathol* 2016;186:733–47.
- Ahmed AA, Wang X, Lu Z, Goldsmith J, Le XF, Grandjean G, et al. Modulating microtubule stability enhances the cytotoxic response of cancer cells to paclitaxel. *Cancer Res* 2011;71:5806–17.
- Ahmed AA, Lu Z, Jennings NB, Etemadmoghadam D, Capalbo L, Jacamo RO, et al. SIK2 is a centrosome kinase required for bipolar mitotic spindle formation that provides a potential target for therapy in ovarian cancer. *Cancer Cell* 2010;18:109–21.
- Rosen DG, Yang G, Deavers MT, Malpica A, Kavanagh JJ, Mills GB, et al. Cyclin E expression is correlated with tumor progression and predicts a poor prognosis in patients with ovarian carcinoma. *Cancer* 2006;106:1925–32.
- Vichai V, Kirtikara K. Sulforhodamine B colorimetric assay for cytotoxicity screening. *Nat Protoc* 2006;1:1112–6.
- Monks A, Scudiero D, Skehan P, Shoemaker R, Paull K, Vistica D, et al. Feasibility of a high-flux anticancer drug screen using a diverse panel of cultured human tumor cell lines. *J Natl Cancer Inst* 1991;83:757–66.
- Chou TC. Drug combination studies and their synergy quantification using the Chou-Talalay method. *Cancer Res* 2010;70:440–6.
- Alama A, Barbieri F, Favre A, Cagnoli M, Novello E, Pedulla F, et al. Establishment and characterization of three new cell lines derived from the ascites of human ovarian carcinomas. *Gynecol Oncol* 1996;62:82–8.
- Wilson AP. Characterization of a cell line derived from the ascites of a patient with papillary serous cystadenocarcinoma of the ovary. *J Natl Cancer Inst* 1984;72:513–21.
- Benard J, Da Silva J, De Blois MC, Boyer P, Duvillard P, Chiric E, et al. Characterization of a human ovarian adenocarcinoma line, IGROV1, in tissue culture and in nude mice. *Cancer Res* 1985;45:4970–9.
- Simon WE, Albrecht M, Hansel M, Dietel M, Holzel F. Cell lines derived from human ovarian carcinomas: growth stimulation by gonadotropic and steroid hormones. *J Natl Cancer Inst* 1983;70:839–45.

Disclosure of Potential Conflicts of Interest

H. Vankayalapati reports receiving other commercial research support from and holds ownership interest (including patents) in Arrien Pharmaceuticals.

No potential conflicts of interest were disclosed by the other authors.

Authors' Contributions

Conception and design: J. Zhou, A. Alfraidi, H. Vankayalapati, Z. Lu, R.C. Bast
Development of methodology: J. Zhou, J.M. Santiago-O'Farrill, A. Alsaadi, A.A. Ahmed, W. Mao, Y. Wang, H. Vankayalapati

Acquisition of data (provided animals, acquired and managed patients, provided facilities, etc.): J. Zhou, S. Zhang, J.M. Santiago-O'Farrill, A. Alsaadi, H. Yang, J. Liu, W. Mao, Y. Wang, H. Vankayalapati, R.C. Bast

Analysis and interpretation of data (e.g., statistical analysis, biostatistics, computational analysis): J. Zhou, A. Alfraidi, S. Zhang, J.M. Santiago-O'Farrill, A.A. Ahmed, H. Yang, W. Mao, Y. Wang, H. Vankayalapati, Z. Lu, R.C. Bast
Writing, review, and/or revision of the manuscript: J. Zhou, A. Alfraidi, H. Vankayalapati, Z. Lu, R.C. Bast

Administrative, technical, or material support (i.e., reporting or organizing data, constructing databases): A. Alfraidi, S. Zhang, H. Takemori, H. Vankayalapati

Study supervision: A. Alfraidi, A.A. Ahmed, J. Liu, H. Vankayalapati, Z. Lu, R.C. Bast

Other (ARN-3236 inhibitor synthesis): V. Krishna Yerramreddy Reddy

Grant Support

This work was supported by the Cancer Prevention and Research Institute of Texas (RP110-595), the NCI at the NIH (P50 CA83639, U54 CA151668, R01 CA135354, P30 CA16672, and UH2 TR000943-01), the Zarrow Foundation, the Mossy Foundation, the National Foundation for Cancer Research, the RGK Foundation, and the generous support of Stuart and Gay Lynne Zarrow.

The costs of publication of this article were defrayed in part by the payment of page charges. This article must therefore be hereby marked *advertisement* in accordance with 18 U.S.C. Section 1734 solely to indicate this fact.

Received June 21, 2016; revised September 10, 2016; accepted September 14, 2016; published OnlineFirst September 27, 2016.

Zhou et al.

16. Miranda F, Mannion D, Liu S, Zheng Y, Mangala LS, Redondo C, et al. Salt-inducible kinase 2 couples ovarian cancer cell metabolism with survival at the adipocyte-rich metastatic niche. *Cancer Cell* 2016;30:273–89.
17. Vankayalapati H, Yerramreddy V, Ganipisetty VB, Talluri S, Appalaneni RP, inventors. Preparation of substituted 1H-pyrrolo[2,3-b]pyridine and 1H-pyrazolo[3,4-b]pyridine derivatives as salt inducible kinase 2 (SIK2) inhibitors. United States patent US 20140256704 A1. 2014 Jun 19.
18. Alfreidi A, Zhang S, Mao W, Wang Y, Takemori H, Lu Z, et al. Highly potent and orally available SIK2 inhibitors block growth of human ovarian cancer cells in culture and xenografts [abstract]. In: Proceedings of the 105th Annual Meeting of the American Association for Cancer Research; 2014 Apr 5–9; San Diego, CA. Philadelphia, PA: AACR; 2014. Abstract nr 749.
19. Lombardi MS, Gillieron C, Dietrich D, Gabay C. SIK inhibition in human myeloid cells modulates TLR and IL-1R signaling and induces an anti-inflammatory phenotype. *J Leukoc Biol* 2016;99:711–21.
20. Screaton RA, Conkright MD, Katoh Y, Best JL, Canetti G, Jeffries S, et al. The CREB coactivator TORC2 functions as a calcium- and cAMP-sensitive coincidence detector. *Cell* 2004;119:61–74.
21. Meraldi P, Nigg EA. The centrosome cycle. *FEBS Lett* 2002;521:9–13.
22. Hinchcliffe EH. The centrosome and bipolar spindle assembly: does one have anything to do with the other? *Cell Cycle* 2011;10:3841–8.
23. Mayor T, Hacker U, Stierhof YD, Nigg EA. The mechanism regulating the dissociation of the centrosomal protein C-Nap1 from mitotic spindle poles. *J Cell Sci* 2002;115:3275–84.
24. Vitale I, Galluzzi L, Castedo M, Kroemer G. Mitotic catastrophe: a mechanism for avoiding genomic instability. *Nat Rev Mol Cell Biol* 2011;12:385–92.
25. Erenpreisa J, Kalejs M, Ianzini F, Kosmacek EA, Mackey MA, Emzish D, et al. Segregation of genomes in polyploid tumour cells following mitotic catastrophe. *Cell Biol Int* 2005;29:1005–11.
26. Zhang M, Mukherjee N, Bermudez RS, Latham DE, Delaney MA, Zietman AL, et al. Adenovirus-mediated inhibition of survivin expression sensitizes human prostate cancer cells to paclitaxel in vitro and in vivo. *Prostate* 2005;64:293–302.
27. Wang S, Huang X, Lee CK, Liu B. Elevated expression of erbB3 confers paclitaxel resistance in erbB2-overexpressing breast cancer cells via upregulation of Survivin. *Oncogene* 2010;29:4225–36.
28. Wang Z, Takemori H, Halder SK, Nonaka Y, Okamoto M. Cloning of a novel kinase (SIK) of the SNF1/AMPK family from high salt diet-treated rat adrenal. *FEBS Lett* 1999;453:135–9.
29. Dentin R, Liu Y, Koo SH, Hedrick S, Vargas T, Heredia J, et al. Insulin modulates gluconeogenesis by inhibition of the coactivator TORC2. *Nature* 2007;449:366–9.
30. Horike N, Kumagai A, Shimono Y, Onishi T, Itoh Y, Sasaki T, et al. Downregulation of SIK2 expression promotes the melanogenic program in mice. *Pigment Cell Melanoma Res* 2010;23:809–19.
31. Sasaki T, Takemori H, Yagita Y, Terasaki Y, Uebi T, Horike N, et al. SIK2 is a key regulator for neuronal survival after ischemia via TORC1-CREB. *Neuron* 2011;69:106–19.
32. Bricambert J, Miranda J, Benhamed F, Girard J, Postic C, Dentin R. Salt-inducible kinase 2 links transcriptional coactivator p300 phosphorylation to the prevention of ChREBP-dependent hepatic steatosis in mice. *J Clin Invest* 2010;120:4316–31.
33. Nagel S, Leich E, Quentmeier H, Meyer C, Kaufmann M, Zaborski M, et al. Amplification at 11q23 targets protein kinase SIK2 in diffuse large B-cell lymphoma. *Leuk Lymphoma* 2010;51:881–91.
34. Imielinski M, Berger AH, Hammerman PS, Hernandez B, Pugh TJ, Hodis E, et al. Mapping the hallmarks of lung adenocarcinoma with massively parallel sequencing. *Cell* 2012;150:1107–20.
35. Bon H, Wadhwa K, Schreiner A, Osborne M, Carroll T, Ramos-Montoya A, et al. Salt-inducible kinase 2 regulates mitotic progression and transcription in prostate cancer. *Mol Cancer Res* 2015;13:620–35.
36. Domcke S, Sinha R, Levine DA, Sander C, Schultz N. Evaluating cell lines as tumour models by comparison of genomic profiles. *Nat Commun* 2013;4:2126.
37. Gonczy P. Centrosomes and cancer: revisiting a long-standing relationship. *Nat Rev Cancer* 2015;15:639–52.
38. Chan JY. A clinical overview of centrosome amplification in human cancers. *Int J Biol Sci* 2011;7:1122–44.
39. Kawamura E, Fielding AB, Kannan N, Balgi A, Eaves CJ, Roberge M, et al. Identification of novel small molecule inhibitors of centrosome clustering in cancer cells. *Oncotarget* 2013;4:1763–76.
40. Kwon M, Godinho SA, Chandhok NS, Ganem NJ, Azioune A, Thery M, et al. Mechanisms to suppress multipolar divisions in cancer cells with extra centrosomes. *Genes Dev* 2008;22:2189–203.

Clinical Cancer Research

A Novel Compound ARN-3236 Inhibits Salt-Inducible Kinase 2 and Sensitizes Ovarian Cancer Cell Lines and Xenografts to Paclitaxel

Jinhua Zhou, Albandri Alfraidi, Shu Zhang, et al.

Clin Cancer Res 2017;23:1945-1954. Published OnlineFirst September 27, 2016.

Updated version Access the most recent version of this article at:
[doi:10.1158/1078-0432.CCR-16-1562](https://doi.org/10.1158/1078-0432.CCR-16-1562)

Supplementary Material Access the most recent supplemental material at:
<http://clincancerres.aacrjournals.org/content/suppl/2017/03/10/1078-0432.CCR-16-1562.DC1>

Cited articles This article cites 38 articles, 7 of which you can access for free at:
<http://clincancerres.aacrjournals.org/content/23/8/1945.full#ref-list-1>

Citing articles This article has been cited by 4 HighWire-hosted articles. Access the articles at:
<http://clincancerres.aacrjournals.org/content/23/8/1945.full#related-urls>

E-mail alerts [Sign up to receive free email-alerts](#) related to this article or journal.

Reprints and Subscriptions To order reprints of this article or to subscribe to the journal, contact the AACR Publications Department at pubs@aacr.org.

Permissions To request permission to re-use all or part of this article, use this link
<http://clincancerres.aacrjournals.org/content/23/8/1945>.
Click on "Request Permissions" which will take you to the Copyright Clearance Center's (CCC) Rightslink site.